

# Arc-scanning Very High-frequency Digital Ultrasound for 3D Pachymetric Mapping of the Corneal Epithelium and Stroma in Laser in situ Keratomileusis

Dan Z. Reinstein, MD, MA(Cantab), FRCSC; Ronald H. Silverman, PhD; Tatiana Raevsky, MS; George J. Simoni, BEng; Harriet O. Lloyd, BS; David J. Najafi, MD; Mark J. Rondeau; D. Jackson Coleman, MD

## ABSTRACT

**PURPOSE:** To test and demonstrate measurement precision, imaging resolution, 3D thickness mapping, and clinical utility of a new prototype 3D very high-frequency (VHF) (50 MHz) digital ultrasound scanning system for corneal epithelium, flap, and residual stromal thickness after laser in situ keratomileusis (LASIK).

**METHODS:** VHF ultrasonic 3D data was acquired by arc-motion, meridional scanning within a 10-mm zone. Digital signal processing techniques provided high-resolution B-scan imaging, and I-scan traces for high-precision pachymetry in 4 eyes. Thickness maps of individual corneal layers

were constructed. Reproducibility of epithelial, flap, and full corneal pachymetry was assessed for single-point and 3D thickness mapping by repeated measures. Thickness mapping of the epithelium, stroma, flap, and full cornea were determined before and after LASIK. Preoperative to postoperative difference maps for epithelium, flap, and stroma were produced to demonstrate anatomical changes in the thickness profile of each layer.

**RESULTS:** Surface localization precision was 0.87  $\mu\text{m}$ . Central reproducibility for single-point pachymetry of epithelium was 0.61  $\mu\text{m}$ ; flap, 1.14  $\mu\text{m}$ ; and full cornea, 0.74  $\mu\text{m}$ . Reproducibility for central pachymetry on 3D thickness mapping was 0.5  $\mu\text{m}$  for epithelium and 1.5- $\mu\text{m}$  for full cornea. B-scans and 3D thickness maps after LASIK demonstrated resolution of epithelial, stromal component of the flap, and residual stromal layers. Large epithelial profile changes were demonstrated after LASIK. Topographic variability of flap thickness and residual stromal thickness were significant.

**CONCLUSIONS:** VHF digital ultrasound arc-B scanning provides high-resolution imaging and high-precision three-dimensional thickness mapping of corneal layers, enabling accurate anatomical evaluation of the changes induced in the cornea by LASIK. [*J Refract Surg* 2000;16:414-430]

*From the Margaret M. Dyson Vision Research Institute, Department of Ophthalmology, Weill Medical College of Cornell University, New York, NY (Reinstein, Silverman, Simoni, Lloyd, Najafi, Rondeau, Raevsky, and Coleman), the Department of Ophthalmology, University of British Columbia, Vancouver, BC, Canada (Reinstein), Lasik Vision Corporation, Vancouver, BC, Canada (Reinstein), and the Faculté de Médecine St. Antoine, Université Paris VI – Centre Hospitalier National d’Ophtalmologie des Quinze-Vingts, Paris, France (Reinstein).*

*Supported in part by NIH grant EY01212, the Dyson Foundation, the St. Giles Foundation and Research to Prevent Blindness, Inc.*

*Certain aspects of the ultrasound technology described in this report are protected by U.S. and international patents. Patents are administered by the Cornell Research Foundation, Ithaca, New York.*

*The following authors have a proprietary interest in materials presented: Reinstein, Silverman, Raevsky, Simoni, Lloyd, Rondeau, and Coleman.*

*Preparation in partial fulfillment of the requirements for the doctoral thesis, University of Cambridge, for Dr. Reinstein.*

*Correspondence: Dan Z Reinstein, MD, MA(Cantab), FRCSC, Department of Ophthalmology, Weill Medical College of Cornell University, 1300 York Ave., Rm A-855, New York, NY 10021. Fax: 212.746.8135; E-mail: dZR@boodle.med.cornell.edu*

*Received: February 24, 2000*

*Accepted: June 12, 2000*

Corneal excimer laser refractive surgery today is based on ocular refraction, not on corneal anatomy. Spectacle correction is used to determine the volume of tissue that needs to be removed from the cornea to produce the desired refractive change. A large discrepancy exists between the known accuracy of the excimer laser at removing corneal tissue and the accuracy of the refractive results of photorefractive keratectomy

(PRK) or laser in situ keratomileusis (LASIK). Known factors for this discrepancy include inaccuracy in the stromal ablation rate<sup>1</sup>, inaccuracy in refraction<sup>2</sup>, and inconsistent surgical technique. Recent interest in flattening the three-dimensional (3D) wave-front aberration function aims to improve surgical accuracy and visual quality (higher order visual aberrations).<sup>3</sup> However, as the accuracy of correction for the first order polynomial expansion terms (representing sphere and cylinder) is currently limited, claims to correct higher order aberrations are premature. It is becoming increasingly apparent that to improve the accuracy of corneal refractive surgery, anatomical elements, such as epithelial dynamics and biomechanical changes within the cornea need to be considered.<sup>4</sup>

Current methodology for determination of corneal anatomy to define the shape of the front and back surfaces of the cornea primarily involves use of optical topographical methods. At present, these elements are used in the detection of corneal abnormalities during screening of potential candidates but not the execution of routine refractive surgical protocols. Most refractive surgeons today still rely upon corneal topography performed for the front surface of the cornea only, despite the commercially available Orbscan (Orbtek/Bausch & Lomb, Salt Lake City, UT), a slit-beam topographical system that maps both the anterior and posterior corneal surfaces.

Despite these advances in corneal topography, it is not always possible to diagnose the cause of subjective visual complaints by topography alone.<sup>5</sup> Visual complications can be due to internal corneal refractive interfaces (such as the epithelial-stromal interface) that do not show up as a surface abnormality detectable by videokeratography.<sup>5</sup> With burgeoning surgical rates of PRK and LASIK worldwide, it is becoming increasingly evident that there is a need for a method of determining the layered anatomy of the changes responsible for optical complications—one that would allow true anatomical diagnoses to be made and more cognitive surgical planning to be performed.

The importance of epithelial changes in corneal refractive surgery has probably been underestimated. Significant changes in epithelial thickness profiles in both PRK<sup>6</sup> and LASIK<sup>5,7</sup> have been demonstrated and implicated in myopic regression. The curvature of Bowman's layer in the center of the normal cornea is on the average greater than that of the epithelial surface.<sup>8</sup> Since the refractive index of epithelium and stroma are sufficiently different (1.401 vs. 1.377)<sup>9</sup>, the epithelial-stromal interface

constitutes an important refractive interface within the cornea, with a mean power contribution estimated at approximately -3.60 diopters (D).<sup>8</sup> Thus, changes in the epithelial lenticule occurring after surgery will result in unplanned refractive shifts. This is probably one of the reasons why current ablation depths and profiles (nomograms) differ from theoretical ablation profiles—they incorporate the average change of epithelial power for a given level of stromal surface change (level of myopia or hyperopia treated). If epithelial dynamics were found to follow a predictable pattern, this knowledge could be used to improve the accuracy of outcomes.

In LASIK, the creation of a flap and subsequent removal of stroma leads to other significant questions regarding surgical accuracy and safety.<sup>10</sup> The thickness of the flap determines at what level stromal tissue removal commences, and it is directly related to the amount of stromal tissue remaining in the posterior cornea under the flap after surgery. This may be a factor in refractive accuracy due to biomechanical changes. A thinner flap is more difficult to handle surgically. A thicker flap leaves less tissue in the bed after LASIK.

In 1993, we reported the first confirmed measurement of the epithelium of the cornea *in vivo* using very high-frequency (VHF) ultrasound. We demonstrated that acoustic interfaces detected were indeed located spatially at the epithelial surface and the interface between epithelial cells and the surface of Bowman's layer.<sup>11</sup> We also reported the first high-precision VHF 3D epithelial thickness mapping system.<sup>12</sup> This system, acquiring a series of parallel, rectilinear B-scans, was capable of mapping the epithelial layer thickness within the central 3 to 4-mm area. By using digital signal processing techniques (I-scan), a 2.0  $\mu\text{m}$  reproducibility for epithelial thickness measurements was obtained.<sup>13</sup> The I-scan is an A-scan-like trace, produced by digital processing of the stored radiofrequency ultrasonic data. The I-scan trace represents the instantaneous energy intensity with time as compared to the average amplitude represented by the conventionally employed A-scan. Previous studies demonstrated that the I-scan more than doubles the measurement precision afforded by the analog A-scan process.<sup>13</sup> Recently, by increasing the fidelity of the digitized signal, we further improved the epithelial thickness measurement precision to 1.3  $\mu\text{m}$ .<sup>5</sup> This system has been used to characterize central epithelial anatomy and demonstrate that the power of the epithelium may not be constant from eye to eye.<sup>14</sup> We also examined the shape of Bowman's layer<sup>8</sup>, the

measurement of anterior corneal scars for planning therapeutic keratectomy<sup>15,16</sup>, the quantitative analysis of corneal scarring (haze) after PRK<sup>17</sup>, and the measurement of the depth of radial keratotomy incisions.<sup>18</sup> We reported on the analysis of epithelial and stromal changes after lamellar corneal surgery, demonstrating significant epithelial changes after uncomplicated LASIK and the masking of stromal surface irregularities that were producing optical complications.<sup>5</sup>

Here, we present a new prototype VHF reverse arc-B scanning system, designed to increase the corneal acquisition area to a 10-mm zone in a multi-meridional fashion. The new system was designed to produce high-resolution B-scans of the cornea and enable thickness measurements of the epithelium, flap, and residual stromal layer in LASIK. We also set out to determine the point surface localization precision and the two-dimensional (combined axial and lateral) reproducibility of 3D thickness mapping.

**PATIENTS AND METHODS**

Ultrasound scanning was performed in two patients to determine the reproducibility of z-axis (axial) surface localization, the one-point pachymetric reproducibility, and the pachymetric reproducibility on thickness mapping. Two other patients were scanned to demonstrate the two-dimensional cross-sectional B-scan appearance of the cornea before and after LASIK and the 3D pachymetric anatomy and changes in the cornea before and after LASIK.

**Patients**

This study conformed to the tenets of the Declaration of Helsinki and patients were scanned only after giving fully informed consent. A complete ocular examination including manifest refraction, videokeratographic mapping (TMS-1; Tomey Technologies, Inc., Cambridge, MA) and Orbscan mapping was performed to screen for corneal abnormalities and determine patient candidacy for refractive surgery. VHF ultrasound scanning was per-

formed before and after LASIK surgery as described below.

Four patients were recruited and one eye from each patient was scanned. The right eye of patient #1 was scanned 4 months after uneventful LASIK for point-reproducibility studies. The right unoperated cornea of patient #2 was scanned for two-dimensional pachymetric reproducibility studies. The right cornea of patient #3 was scanned to demonstrate the B-scan imaging appearances before and 6 months after LASIK. The left eye of patient #4 was scanned in 3D for layered analysis of the cornea before and after LASIK.

LASIK procedures were carried out using either the Hansatome microkeratome (Bausch & Lomb, Irvine, CA) with a superior hinge using the 8.5-mm ring and the 160-µm head, or the Moria LSK-One microkeratome (Moria, France) with a nasal hinge using the “0” suction ring and the “130” (160-µm) head. Excimer laser ablation was carried out with either the Bausch & Lomb Technolas 217 or the Nidek EC-5000 (Nidek Co. Ltd., Gamagori, Japan) excimer laser. A summary of the patients and procedure parameters is shown in Table 1.

**Ultrasound Scanning and Analysis**

**Patient Preparation**—The scanning system and patient setup is shown in Figure 1. For scanning, patients were placed in the supine position. A standard eye immersion waterbath was set up using a 1020 Steri-Drape (3M Health Care, St. Paul, MN) and a ring-stand. Sterile normal saline (at 33° C) was used as the acoustic coupling medium between the eye and the transducer. By use of a plum-bob and a periscope, the visual axis of eye not being scanned was placed vertically below a blinking fixation target on the ceiling 3 meters above. This provided vertical alignment of both visual axes as well as fixation of the eye during the scan sequence.

**Scanning System and Procedure**—Our system consists of a high-frequency (50 MHz) broadband transducer (Panametrics, Inc., Waltham, MA) mounted on a mechanical reverse-arc motion controller. The mount enables the focus of the

**Table 1  
Population and Procedures**

Patient No.	Eye and Procedure	Purpose	Microkeratome	Excimer Laser	Time after LASIK
1	OD-LASIK	One-point reproducibility	Hansatome	Technolas 217	6 months after surgery
2	OS-None	3D reproducibility	N/A	N/A	Unoperated
3	OD-LASIK	2D B-scan imaging	Moria One	Nidek EC-5000	4 months after surgery
4	OS-LASIK	3D layered corneal anatomy before and after LASIK	Moria One	Nidek EC-5000	6 months after surgery

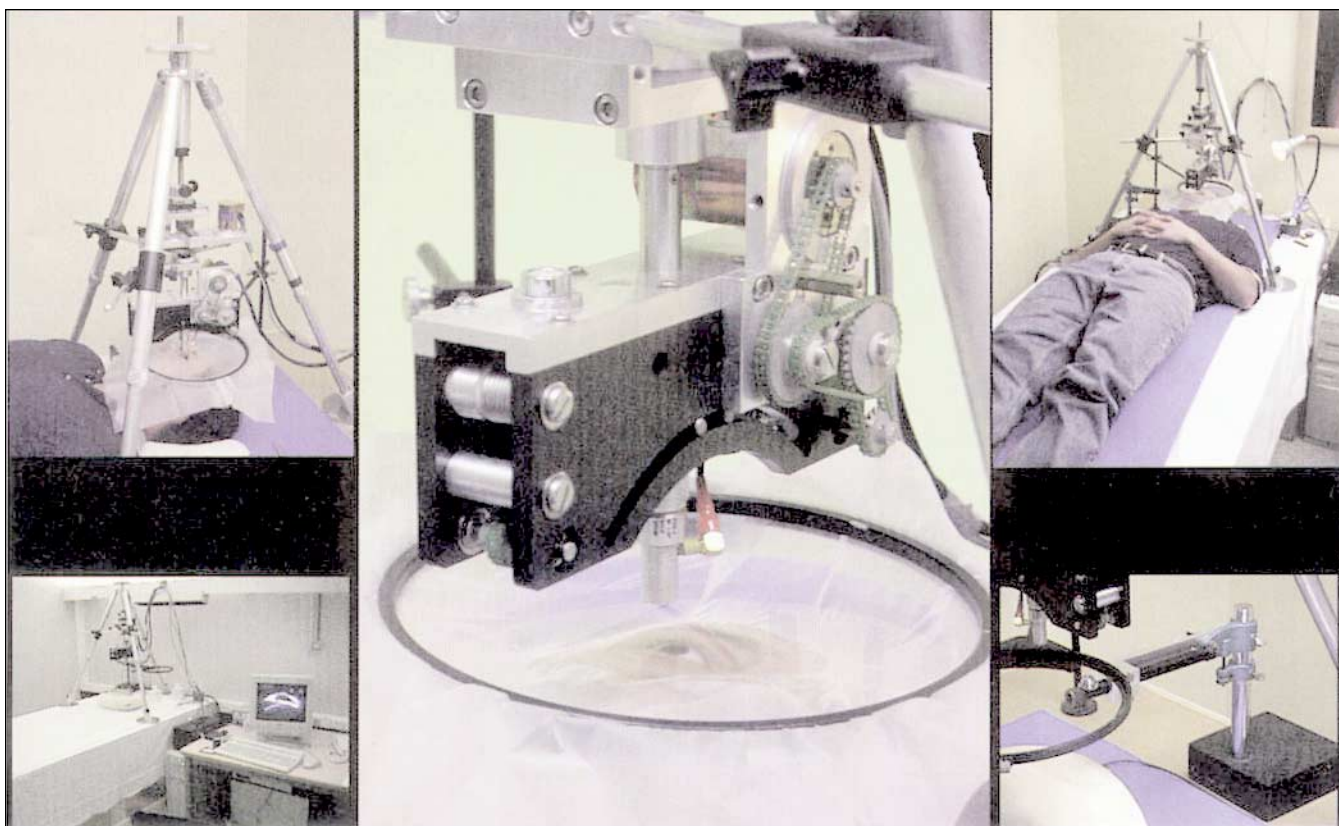


**Figure 1.** Photographs of scanner and patient setup. The transducer is shown in a central vertical position within the arc-motion (center). The motion controller is set under a reverse-tripod on the scanning table with the computer control system adjacent (bottom left). The eye is placed in a standard immersion saline bath, the eye being scanned under the transducer while the other eye (behind the drape) is looking through a vertical axis periscope (bottom right) around the equipment and up to a fixation target on the ceiling (not shown).

transducer to sweep an arc segment of cornea following the corneal contour and enabling ultrasonic data to be acquired over an area 8 to 10-mm in diameter.<sup>19</sup> For scanning, the ultrasound transducer axis was aligned in the vertical axis by use of a fluid level, and the ultrasound beam focus (12 mm) was placed on the cornea under real-time oscilloscope visualization of the echo trace. Either M-mode or B-mode scans were obtained (see below). For 3D scan sets, the scan sequence consisted of 5 meridional scans at 45° intervals (the first and last meridians were the same). Each scan sweep took approximately 0.5 seconds. During the acquisition of each scan, data were converted (in near real-time) to a B-scan displayed on the control-computer screen. Each B-scan reveals information regarding centration, ranging, and eye-movements that may have occurred during the scan sweep. The examiner either accepted or chose to repeat a particular meridional sweep before proceeding to the next. Each scan consisted of up to 512 scan lines or pulse echo vectors (at approximately 0.1° intervals). The full 3D scan sequence took approximately 12 sec-

onds to acquire. The standard eye-immersion water-bath took approximately 1 minute to set up in each eye.

**Data Analysis**—Scan data were digitized during a 10-microsecond window at a rate of 500 MHz and stored for subsequent processing to B-scan images for visualization and I-scan traces for biometry. Digital signal processing (deconvolution and determination of the signal envelope by analytic signal magnitude detection) to I-scans<sup>13</sup> was used to detect corneal tissue interfaces along each pulse-echo vector. The time-based distances between I-scan peaks were converted to microns using the speed of sound constant for cornea of 1640-m/s.<sup>20</sup> Localization of each interface peak along each scan line within the B-scan was achieved by an interactive semi-automatic expert system.<sup>21</sup> The positional localization of each peak was hence achieved in a 3D coordinate system according to the meridian of the B-scan, the scan line within the B-scan, and the axial (radial) location of the peak within the B-scan. Surface point coordinates from all interfaces were stored in matrix format and used for reconstruction of the acoustic interfaces in 3D. The thickness of

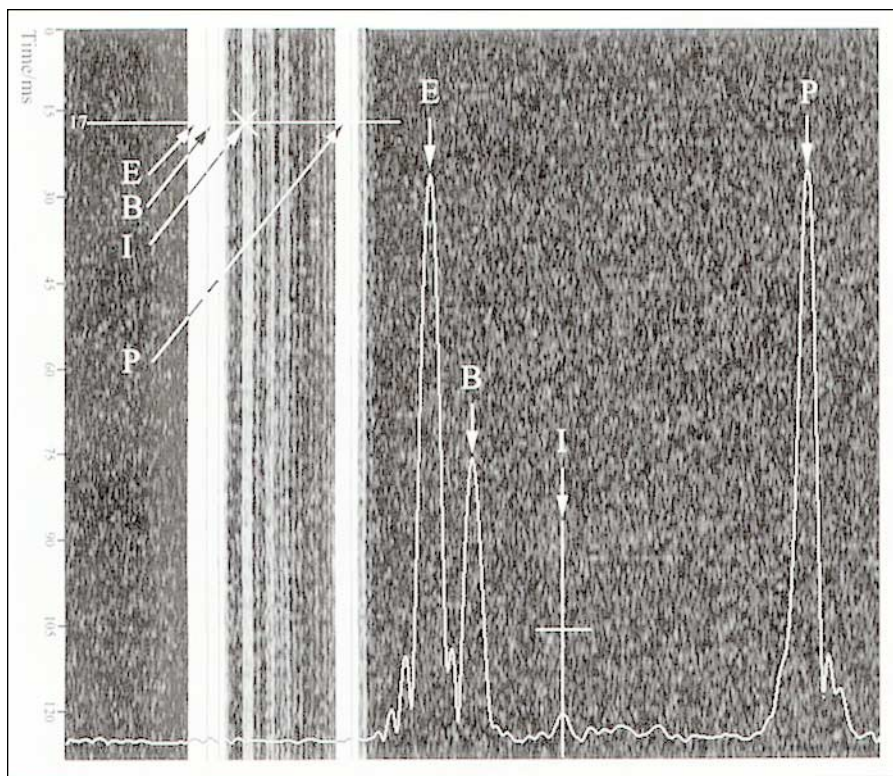


**Figure 2.** M-scan from the central cornea of a patient 6 months after uneventful LASIK. The image consists of 128 (horizontal) scan lines taken at 1 millisecond intervals. Each scan line represents a temporally displaced pulse echo vector from the same corneal location. Scan line 17 is indicated by the analytical software as is the resulting I-scan plot derived by analysis. Peaks on the I-scan plot correspond to acoustic interfaces along the scan line echo vector. The first peak (E) corresponds to the saline-epithelial interface, the second peak (B) to the epithelial-Bowman's interface, the third peak (I) to the location of the lamellar interface, and the fourth peak (P) to the interface between the posterior cornea and aqueous. The time-based interval between peaks is converted to distance by using the speed of sound constant for cornea (1640-m/s). The stromal bed beneath the flap demonstrates slightly increased ultrasonic backscatter relative to the stroma of the flap.

each layer was then derived from the distance between surfaces in the radial direction (perpendicular to the back surface of the cornea).<sup>22</sup> A simple linear polar/radial interpolation function was used to interpolate between scan meridians.

For plotting of thickness mapping we imported the above data-matrix into Deltagraph v.4.5 for Macintosh (SPSS Inc., Richmond, CA). Surface fill plots X,Y,Z were employed to display thickness data on a color scale. Color scales were subjectively adjusted to delineate the variability in thickness profile of the corneal layer in question.

#### Reproducibility Studies

**Point Localization Precision**—To test the point surface localization precision of the system, the transducer beam was focused perpendicularly onto the vertex of the right cornea of patient #1, who had undergone LASIK 6 months previously (Table 1). Four M-scans were acquired from this central corneal position; each consisted of 128 pulse-echo vectors acquired quasi-instantaneously at a rate of 1 per millisecond. Each M-scan was obtained after removing and repositioning the transducer to the central apical location of the cornea. The time-based distance from the transducer to the epithelial surface was measured by means of the I-scan in each of

the 128 vectors. The standard deviation of the root-mean-square distance was calculated to describe the surface point-localization reproducibility.

**Single-point Pachymetric Precision**—To test the single-point pachymetric reproducibility, the four M-scans obtained from the central corneal region were analyzed by I-scan. The epithelial, flap, and full corneal thickness measurements obtained along the 128 vectors of each M-scan were used to determine the reproducibility of pachymetric measurement of each layer (the standard deviation of repeated measurements of the same location). The reproducibility obtained within each of the four M-scans was averaged to produce a mean reproducibility for each layer as well as an overall mean reproducibility and 95% confidence interval for all layers combined.

**Topographical Pachymetric Precision**—To test the two-dimensional (simultaneous axial and lateral) reproducibility of epithelial and corneal thickness measurements *in vivo*, ten 3D scan sets were obtained sequentially from the right eye of a normal patient. Pachymetric maps of the epithelial layer and full cornea were produced for each of the ten 3D scan sets. Next, the standard deviation was calculated point by point on each pachymetric map for the average value of the ten epithelial thickness

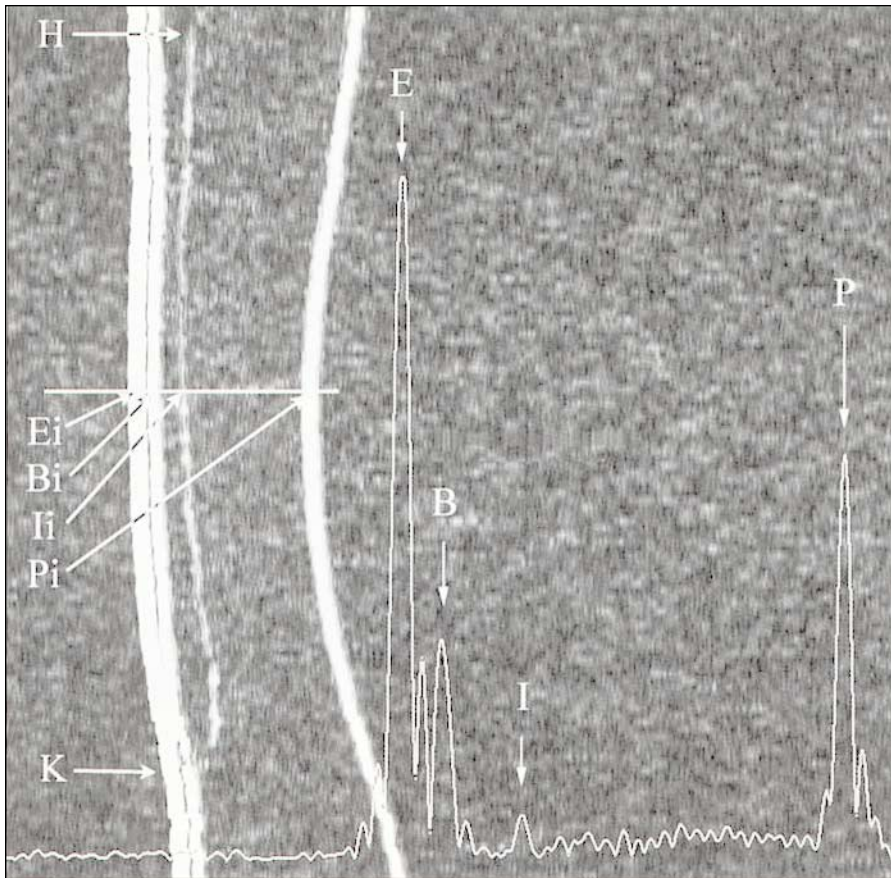


**Figure 3.** Non-geometrically corrected B-scan of a cornea 4 months after LASIK. The scan was performed in the visual axis in the horizontal plane. The B-scan is constructed of 128 pulse echo vectors stacked horizontally. There is a large z-axis zoom in scale (2-mm represented horizontally on the image) relative to the lateral distance (9-mm represented vertically on the image). The B-scan demonstrates interfaces detected ultrasonically for the epithelial surface (Ei), the surface of Bowman's layer (Bi), the lamellar interface (Ii), and the endothelial/posterior corneal surface (Pi). The point of entry of the keratome is demonstrated temporally (K) with a gap of approximately 30  $\mu\text{m}$  in the apposition of Bowman's layer at the site of the original wound. The keratome track is seen to coarse from temporal to nasal, with a depth that decreased from temporal to centrally, then coursing deeper nasally and ending suddenly at the flap hinge (H). Superimposed on the Figure is the I-scan derived by digital processing of the radio frequency ultrasonic B-scan data. The I-scan demonstrates sharp distinct peaks representing the acoustic interfaces of saline-epithelium (E), epithelium-Bowman's (B), the lamellar interface (I), and the endothelial-aqueous interface (P).

values, measured at each local point. From the data, a plot of local standard deviation was derived for epithelial and corneal thickness mapping. This map of local standard deviation represented the 3D reproducibility of repeated measures for the entire process *in vivo*.

## RESULTS

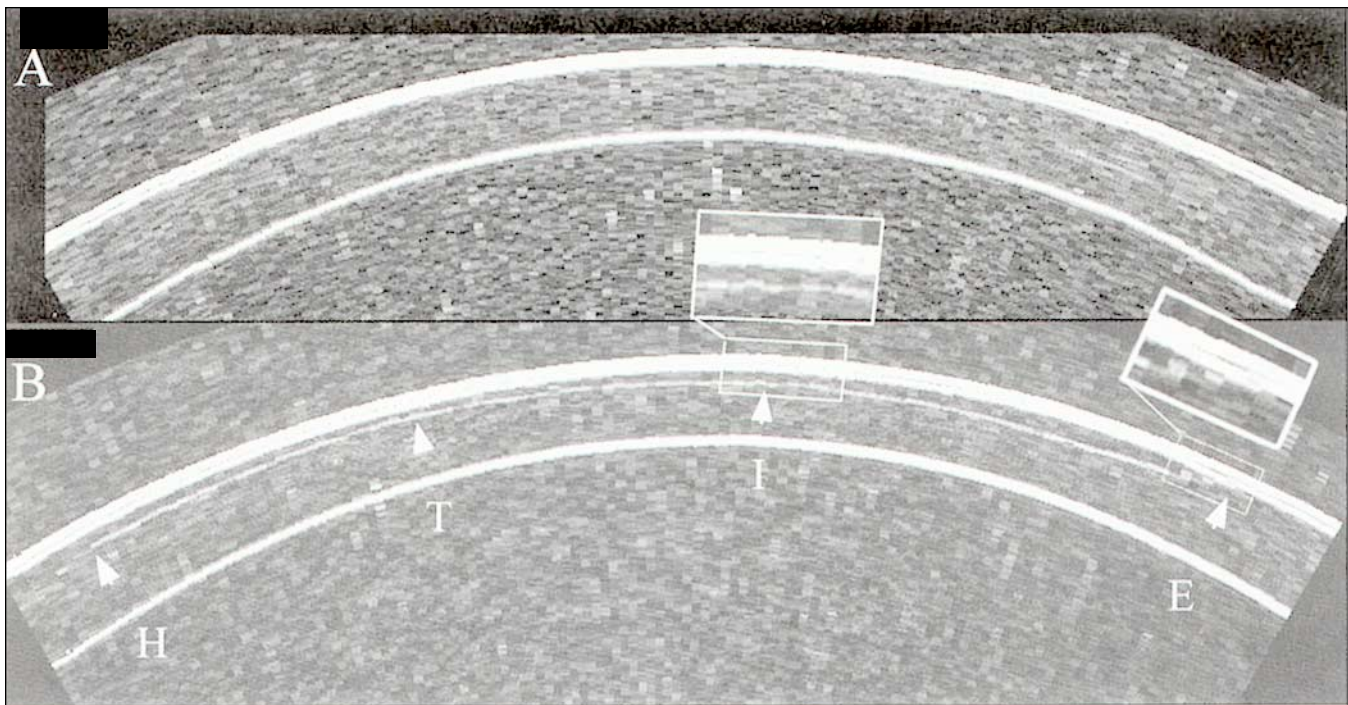
### Single Point-axial Localization Precision

Figure 2 shows an M-scan taken from the central cornea of patient #1, 6 months after LASIK. The image is constructed from stacked 128 horizontal lines. Each scan line represents a pulse-echo sequence. The first scan line was taken at time point zero, and each subsequent scan line (from top to bottom) was taken at consecutive 1-millisecond intervals. Superimposed over the M-scan image is the I-scan trace derived by analysis of the digitized radio-frequency ultrasonic data corresponding to the scan line indicated on the M-scan by a horizontal line. The peaks of the I-scan correspond to the surface of the epithelium, the interface between epithelium and Bowman's layer<sup>11</sup>, the lamellar interface, and the acoustic interface between endothelium and the aqueous humor. The 128 scan

vectors were acquired and digitized within 128 milliseconds so that the assumption can be made that there were negligible eye movements during the acquisition phase. The root-mean-square of the range of the epithelial surface from the transducer, as measured by the I-scan peak, was 12,200  $\mu\text{m}$ . The standard deviation of repeated measurements of the range of the epithelial surface from the transducer was 0.87  $\mu\text{m}$ . Thus, the axial point-localization precision of the system was found to be 0.87  $\mu\text{m}$ .

### Single Point Pachymetric Precision

The standard deviations of the mean epithelial thickness measured at the same location on each of the four M-scans were 0.81, 0.46, 0.85, and 0.30- $\mu\text{m}$  with a mean of 0.61  $\mu\text{m}$  (SD, 0.27  $\mu\text{m}$ ; 95% confidence limits 0.34 to 0.87). The standard deviations for flap thickness measured within each of the M-scans were 1.24, 1.23, 1.14, and 0.93  $\mu\text{m}$ , with a mean of 1.14  $\mu\text{m}$  (SD, 0.14  $\mu\text{m}$ ; 95% confidence limits 1.00 to 1.28). The standard deviations for full corneal thickness measured within each of the M-scans were 0.77, 0.82, 0.84, and 0.53  $\mu\text{m}$ , with a mean of 0.74  $\mu\text{m}$  (SD, 0.14  $\mu\text{m}$ ; 95% confidence limits 0.60 to 0.88). In summary, the mean single point pachymetric reproducibility was found to be



**Figure 4.** Geometrically corrected horizontal B-scans through the center of a cornea. **A)** Before, and **B)** 4 months after LASIK. The epithelial and posterior corneal boundaries are clearly visualized from one end of the corneal scan to the other, spanning a 9-mm diameter of cornea. After LASIK, the additional acoustic interface produced by the interface between the stromal component of the flap and posterior residual stroma is clearly visualized along its entire trajectory; this interface can be seen with an entrance track temporally (E), coursing nasally, first deepening and then becoming more superficial (T) until finally coming to a stop at the flap hinge (H). The keratome entrance point, with a small separation in the cut ends of Bowman's layer under the epithelium, is evident (E); a small irregularity in the smoothness of the keratome track can be appreciated (I).

0.61  $\mu\text{m}$  for epithelium, 1.14  $\mu\text{m}$  for flap, and 0.74  $\mu\text{m}$  for full corneal thickness measurements.

#### B-scan Display of the Cornea

Figure 3 demonstrates the raw (non-geometrically corrected) arc B-scan produced from the scan data of the right cornea of patient #3, 4 months after LASIK. The cornea appears relatively flat or straight from top to bottom of the image, indicating that the trajectory followed by the scanning arc of the transducer was nearly parallel to the corneal surface. Superimposed on the B-scan image is the I-scan trace derived by analysis of the digitized radio-frequency ultrasonic data, corresponding to the scan line indicated on the B-scan (horizontal line radial to the corneal cross-section). The peaks of the I-scan correspond to acoustic interfaces along the vector (indicated in Fig 3) through the corneal B-scan image centrally. This B-scan is depicted geometrically corrected in Figure 4B.

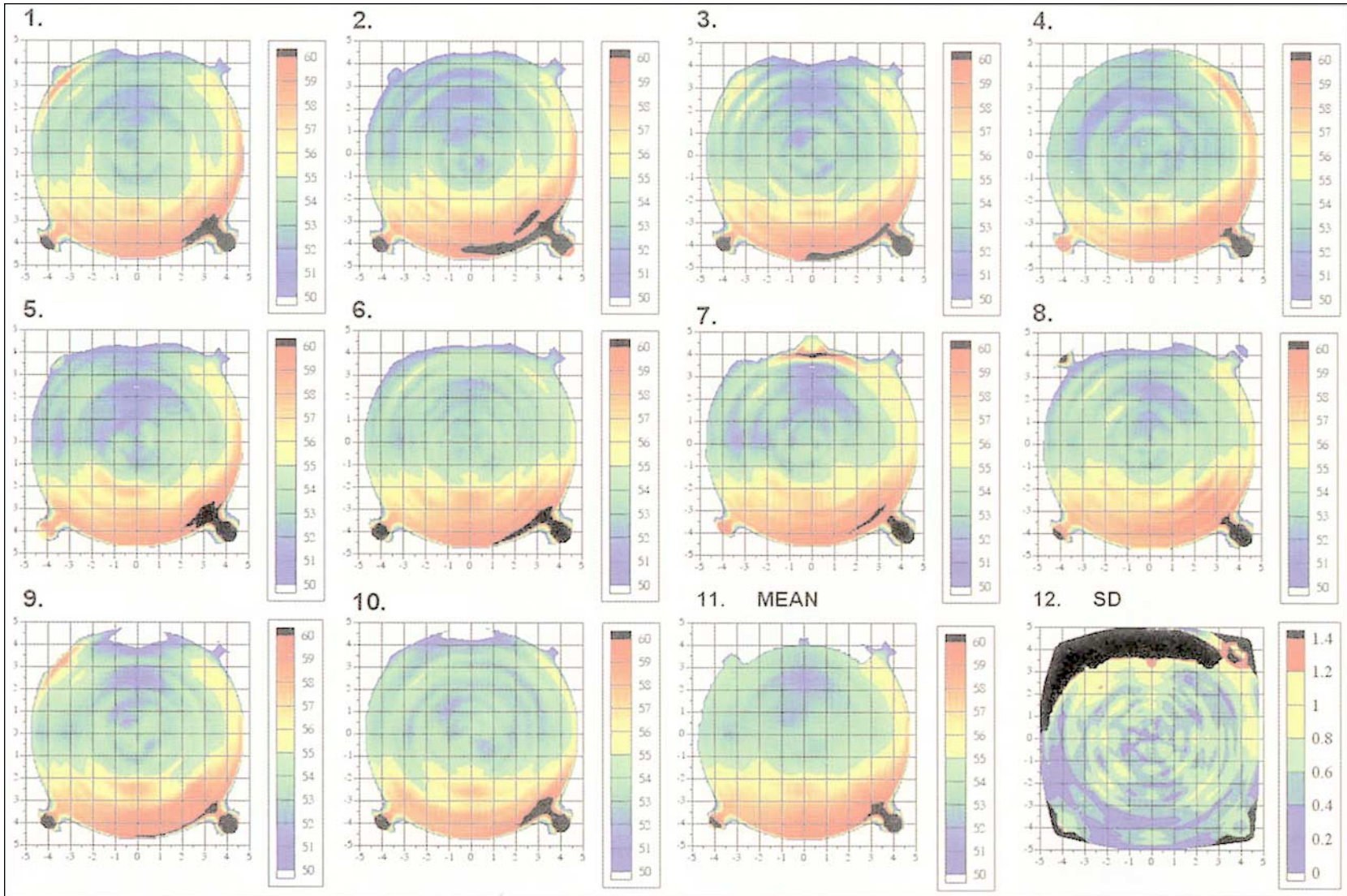
Figure 4 demonstrates a geometrically corrected arc B-scan taken along the horizontal plane of the cornea of the same cornea in Figure 3 (patient #3), before (Fig 4A) and 4 months after

LASIK (Fig 4B). The interfaces of saline-epithelium, epithelium-Bowman's, and the endothelial-aqueous interface are clearly visualized along the 9-mm chord-length of the B-scan preoperatively. After LASIK, the same interfaces are seen with the addition of a distinctly visible keratectomy track.

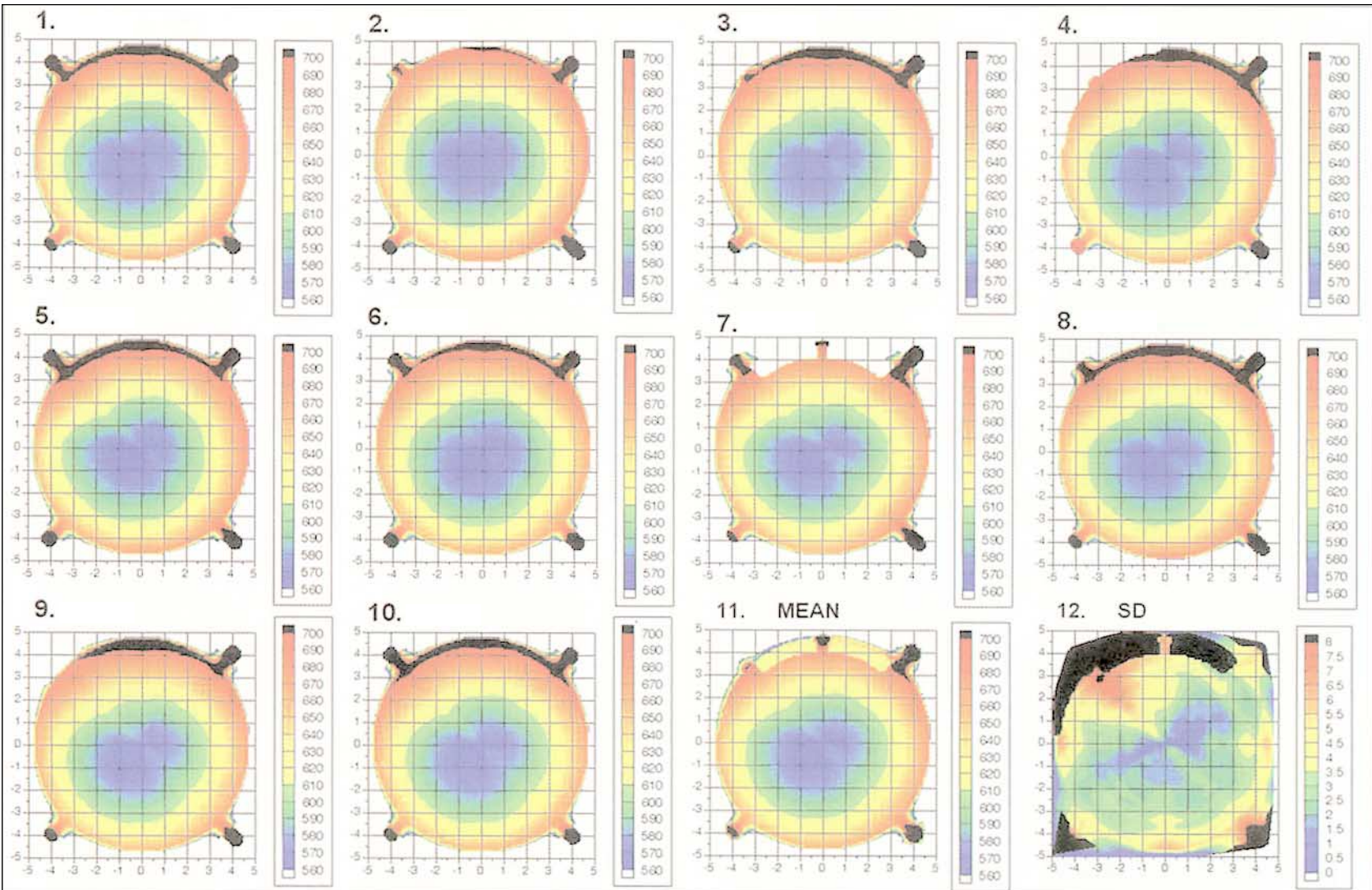
#### 3D Pachymetric Reproducibility

Figure 5 shows 10 pachymetric maps of epithelial thickness produced from the analysis of 10 consecutively acquired multi-meridional 3D B-scan sets of the normal right cornea of patient #2, (Fig 5: maps 1 to 10). Each map depicts the two-dimensional projection of the local epithelial thickness of the cornea represented by a color scale in microns. Gross inspection reveals that the 10 epithelial thickness profiles are qualitatively similar, and the positioning of the color boundaries is remarkably stable from map to map. There is a central epithelial thickness of approximately 54  $\mu\text{m}$ . The epithelial thickness is thinner overlaying the superior cornea (approximately 50  $\mu\text{m}$ ), and thicker overlaying the inferior cornea (approximately 60  $\mu\text{m}$ ).

The two-dimensional mean topographical



**Figure 5.** Ten sequentially obtained epithelial pachymetric maps of the right cornea of a normal patient (maps 1 through 10). All maps are plotted with an identical color scale representing the local epithelial thickness in microns. The maps possess a superimposed Cartesian 1-mm grid with the origin at the center of the corneal map. Map 11 represents the point-by-point two-dimensional mean pachymetric epithelial map for all ten pachymetric maps. Map 12 represents the point-by-point standard deviation topographically for all ten pachymetric maps. Comparison of epithelial thickness maps demonstrates little topographic variation in the thickness profile from map to map. Generally the epithelium is thinner superiorly, and thicker inferiorly. Comparison of each individual epithelial thickness map with the mean of all ten maps shows a good correlation. This map-to-map variability is demonstrated statistically in map 12. The topographic standard deviation (pachymetric reproducibility) in the central 6-mm zone is less than 1  $\mu$ m.



**Figure 6.** Ten sequentially obtained full corneal pachymetric maps of the right cornea of a normal patient (maps 1 through 10). All maps are plotted with an identical color scale representing the local corneal thickness in microns. The lateral scale is represented on a 1-mm grid. Map 11 represents the point-by-point two dimensional mean pachymetric full corneal map for all ten pachymetric maps. Map 12 represents the point-by-point standard deviation topographically for all ten pachymetric maps. Comparing corneal thickness maps, there is little topographic variation in the thickness profile from map to map—all iso-pachymetric contours are similar. Comparison of each individual corneal thickness map with the mean of all ten maps shows high correlation. The map-to-map variability is demonstrated statistically in map 12. The topographic standard deviation (pachymetric reproducibility) varies from scan to scan, with the 45 degree scan demonstrating a higher intrascan reproducibility (approx 1  $\mu\text{m}$ ) than the 135° scan (approximately 5  $\mu\text{m}$  superotemporally). The majority of the central 8-mm zone depicted demonstrates a reproducibility better than 5  $\mu\text{m}$ .

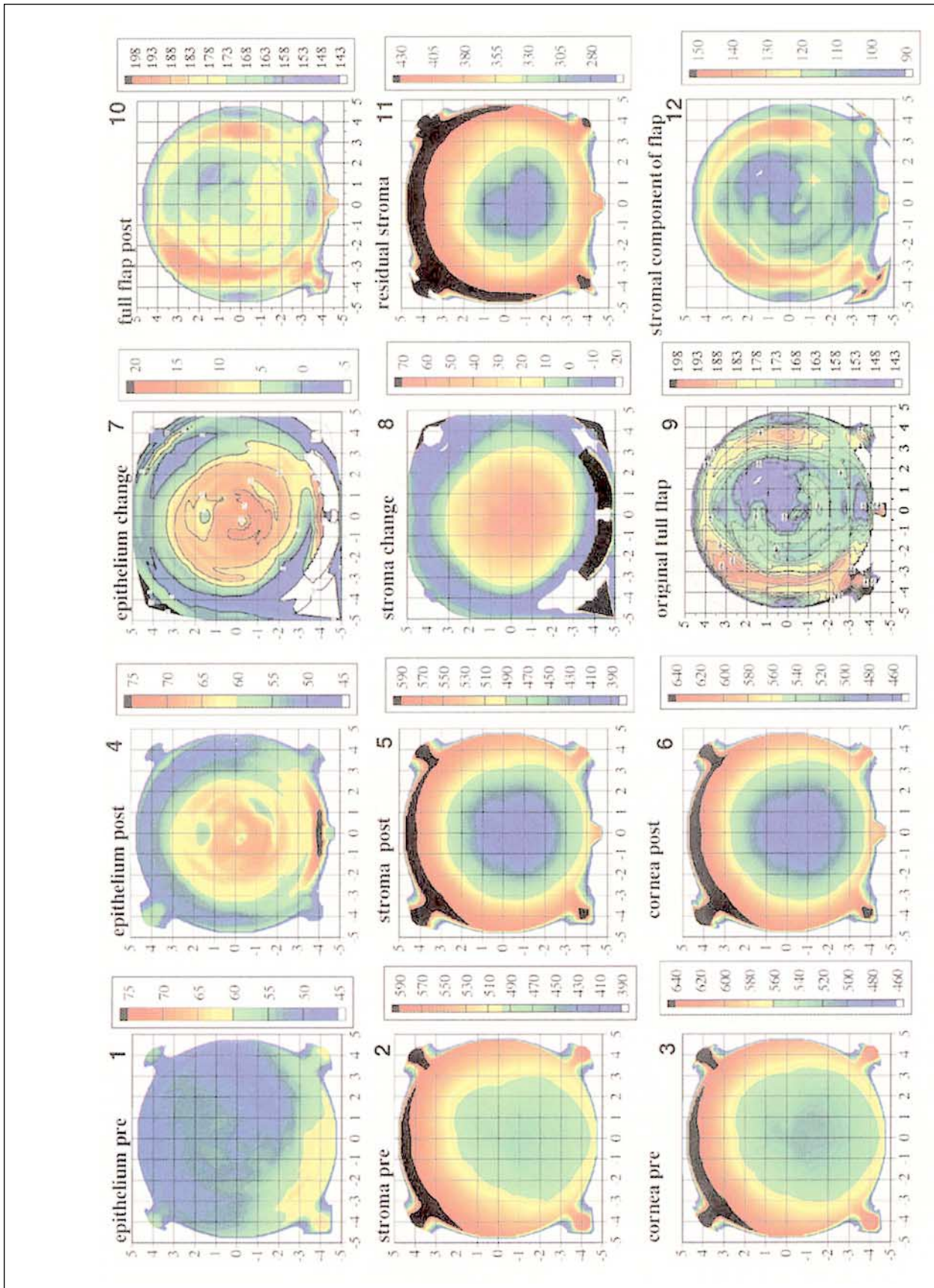


Figure 7. (see page 424)

**Table 2**  
**Summary of the VHF Ultrasound System Precision Characteristics**  
**Standard Deviation of Repeated Measurements at the Same Location**

System Precision Characteristic	Precision (SD of Multiple Measurements) (µm)
Single point axial localization precision for central cornea	
Single point central pachymetric reproducibility for epithelium	0.61
for flap	1.14
for full cornea	0.71
3D pachymetric epithelial reproducibility centrally	0.50
within central 2-mm zone	≤0.6
within central 4-mm zone	≤0.8
within central 8-mm zone	≤1.3
3D pachymetric full cornea reproducibility centrally	≤1.5
within central 2-mm zone	≤4.0
within central 4-mm zone	≤5.5
within central 8-mm zone	≤8.0

thickness of the 10 scan sets is shown in Figure 5 on map 11. As can be seen, the pachymetric profile of each individual epithelial map (maps 1 to 10) is similar to that of the mean profile (map 11). Topographic mapping of the local point-by-point standard deviation of epithelial thickness is shown on map 12. The map of local standard deviation represents the local reproducibility of the entire system/method *in vivo*. The central reproducibility was 0.5 µm. Within the entire 8-mm diameter standard deviation map, the reproducibility remains below 1.3 µm. Within the central 4-mm zone the reproducibility remains at 0.8 µm or better, and within the central 2-mm zone the reproducibility remains at 0.6 µm or better.

Figure 6 shows 10 pachymetric maps of corneal thickness produced from the analysis of the same 10 consecutively acquired multi-meridional 3D B-scan sets as above, by scanning the unoperated

normal right cornea of patient #2, (Fig 6: maps 1 to 10). Each map depicts the two-dimensional projection of the local corneal thickness represented by a color scale in microns. The corneal thickness profiles can be seen to be qualitatively similar with a central corneal thickness of approximately 570 µm, and a thinnest point of approximately 560 µm lying infero-temporal to the center. Topographic mapping of the local point-by-point mean corneal thickness for the 10 scan sets is shown (Fig 6: map 11). The point-by-point standard deviation of epithelial thickness is shown beside this (Fig 6: map 12). Within the central 4-mm zone, the corneal thickness reproducibility remains at 5.5 µm or better, with the majority of the map displaying a reproducibility of 3 µm or better.

A summary of the system reproducibility characteristics is shown in Table 2.

**Figure 7** (see page 423). "C12" display of the cornea of a patient before and 6 months after LASIK OS. The C12 display is set out to be read by temporal grouping (columns) or anatomical grouping (rows). All 12 maps are pachymetric representations of particular corneal layers depicted on a color scale in microns. The preoperative epithelial (1), stromal (2), and full corneal (3) thickness maps appear in the first column. To the right of each of these maps (column two) are the pachymetric maps after LASIK of epithelium (4), stroma (5), and full cornea (6) on identical color scales for direct comparison to the preoperative state. The third column depicts calculated maps only. The calculated epithelial change map (7) is derived by point-by-point subtraction of the preoperative from the postoperative epithelial pachymetric map. Thus, the epithelial change map shows on a color scale the number of microns increase in epithelial thickness after surgery. The area of epithelial thickening is confined to the ablation zone or the zone of surgical corneal flattening. The calculated stromal change map (8) is derived in point-by-point subtraction of the postoperative from the preoperative stromal pachymetric map. Thus the stromal thickness change map shows on a color scale the number of stromal microns decrease due to surgery in a topographic fashion and hence represents the decrease in stromal tissue volume. The calculated map of the original flap (9) is derived by addition of the preoperative epithelial thickness profile (1) to the postoperative stromal component of the flap (12). The postoperative thickness map of the flap (10) includes epithelial changes. The original full flap (9) and postoperative flap (10) are shown on identical color scales for direct comparison. Thickness mapping of the residual stromal layer comprising all stroma beneath and peripheral to the flap is shown in map 11. This map can be critically important in the determination of adequacy of the thickness of the stromal bed for further LASIK enhancement surgery under the flap, because the thinnest point is not always located centrally and may be missed by any form of intraoperative, single-point measurement of the bed.

### 3D Thickness Mapping in LASIK

The right cornea of patient #4 was scanned before and 6 months after LASIK. Preoperative examination revealed a spherical myopia of  $-4.75 -0.25 \times 55^\circ$  with a best spectacle-corrected visual acuity of 20/16. The general preoperative ocular examination was normal. Videokeratographic examination was also normal. At 6 months after LASIK, the cornea was clear with a lamellar interface only faintly detectable in places by slit-lamp microscopy. Uncorrected visual acuity was 20/16 with a residual subjective manifest refraction of plano. Videokeratographic examination showed the customary central flattening with a small surface with-the-rule astigmatism. Layered pachymetric examination of the cornea is shown in Figure 7. This output display of 12 pachymetric maps was designed as a standardized layered pachymetric summary of corneal anatomical changes following LASIK. We chose to name this presentation a "C12" display, for it consists of 12 corneal pachymetric topographical maps of the same cornea. Each map depicts the two-dimensional projection of the local thickness of a given corneal layer represented on a color scale in microns. Within the C12 display, the first column depicts the thickness profiles of the preoperative corneal epithelium (Fig 7: map 1), full stroma (Fig 7: map 2), and full cornea (Fig 7: map 3), respectively. The second column demonstrates the postoperative thickness profiles of the corneal epithelium (Fig 7: map 4), stroma (Fig 7: map 5), and full cornea (Fig 7: map 6). Epithelium, full stroma, and full cornea color scales are identical for preoperative and postoperative stages to allow direct color (thickness) comparison. The third column consists of calculated maps representing topographical epithelial change (Fig 7: map 7) (derived by subtraction of the preoperative from postoperative epithelial map), the stromal change (Fig 7: map 8) (derived by subtraction of the postoperative from preoperative stromal map), and the (calculated) anatomy of the original flap produced at the time of surgery (Fig 7: map 9). The original flap is calculated by adding the stromal component of the flap (Fig 7: map 12) to the *preoperative* epithelial thickness map. The fourth column represents postoperative corneal layers: the thickness profile of the postoperative flap at 6 months (Fig 7: map 10), the 3D thickness profile of the residual stromal layer (stroma excluding the flap), and the postoperative stromal component of the flap (Fig 7: map 12).

The profile map of the preoperative epithelium OS was approximately 9.25 mm in diameter (Fig 7: map 1). The central epithelial thickness was 52  $\mu\text{m}$ .

The epithelium within the 6-mm zone measured temporally between 45 and 57  $\mu\text{m}$ ; nasally this varied between 52 and 64  $\mu\text{m}$ .

The epithelial thickness profile 6 months after LASIK (Fig 7: map 4) demonstrated a central zone of epithelial thickening approximately 7.5 mm in diameter. Within this zone there was a central thickness of 67  $\mu\text{m}$ , which decreased in a concentric fashion to approximately 60  $\mu\text{m}$  at the 6-mm diameter zone. The epithelial change map (Fig 7: map 7) shows the pattern of epithelial thickening and thinning point-by-point. The epithelium thickened from the preoperative state to between 15 and 20  $\mu\text{m}$  centrally, with a concentric decrease in thickening to between 0 and 5  $\mu\text{m}$  at the 7.5-mm diameter zone. Within a 1-mm annulus at the 8-mm diameter zone, there was epithelial *thinning* relative to before LASIK for most of the circumference. We also note that the pattern of epithelial change was such as to increase anterior corneal power (greater tissue addition centrally).

The stromal thickness maps before (Fig 7: map 2) and after LASIK (Fig 7: map 5) are depicted on identical color scales. Note the preoperative inferiorly displaced concentric iso-pachymetric profile both before and after surgery. The stromal change map (Fig 7) on the other hand shows a well centered difference about the center (0,0 coordinate) of the cornea. The difference in stromal thickness from before to after surgery is 70  $\mu\text{m}$  centrally, decreasing to zero at the 7.5-mm diameter zone. Thus, the zone depicted on the color scale from green to red represents the volume of tissue removed from the cornea (assuming no new stromal tissue deposition nor change in stromal density). The predicted central ablation depth by the Nidek EC-5000 excimer laser readout was 73  $\mu\text{m}$  (6.5-mm ablation zone, transition to 7.5 mm). Within the peripheral 8 to 9-mm annular zone there, is a demonstrated stromal thickening of between 10 and 20  $\mu\text{m}$  from before to after LASIK. This finding is unlikely to be an artifact of shifted x-y alignment between the preoperative and postoperative stromal maps, since the finding is symmetrical about the center (0,0 coordinate) of the map. This annulus of stromal thickening coincides with the annulus of epithelial thinning described above.

Examination of the anatomy of the original flap created (Fig 7: map 9) by the Moria LSK-One keratome reveals a central thickness of 158  $\mu\text{m}$ . Within the 4-mm diameter zone, the flap thickness was generally homogeneous between 160 and 165  $\mu\text{m}$  other than for the supero-temporal quadrant where the thickness was lower (decreasing to 145  $\mu\text{m}$ ). The

6 to 7-mm annular zone of the flap possessed an increased thickness to approximately 190  $\mu\text{m}$ . Note that direct measurement of the flap thickness at 6 months (Fig 7: map 10) would not provide an accurate description of the flap anatomy at the time of creation due to the epithelial thickness changes present after LASIK. The stromal component of the flap (Fig 7: map 12) can be seen to possess a thickness profile of approximately 110 to 120  $\mu\text{m}$  within the central 6-mm diameter zone except for the quadrant supero-temporally within the 4-mm diameter zone where this decreased to approximately 95  $\mu\text{m}$ . This area may have been thinner due to the presence of thicker epithelium preoperatively in the corresponding quadrant and the passage of the keratome parallel to the surface of the cornea during applanation by the keratome head.

The 3D thickness profile of the residual stromal layer (Fig 7: map 11) shows a thinnest point of 280  $\mu\text{m}$  approximately 1 mm inferior to the center of the cornea. The iso-pachymetric profile of the residual stromal layer is similar to that of the stroma before and after LASIK but again different from that of the stromal difference map as described above.

**DISCUSSION**

We have demonstrated the use and characteristics of a new very high-frequency digital ultrasound arc-B scanning clinical prototype designed to acquire corneal scan data from 90% to 95% of the corneal diameter in 3D. The system exhibited a single-point surface localization precision of 0.87  $\mu\text{m}$ , a single-point pachymetric precision of under 1  $\mu\text{m}$  for epithelial measurements (0.61  $\mu\text{m}$ ) and corneal thickness measurements (0.71  $\mu\text{m}$ ), and just over 1  $\mu\text{m}$  for flap thickness measurements (1.14  $\mu\text{m}$ ). The system was shown to produce thickness mapping of the corneal epithelium, stromal component of the flap, and residual stromal layer after LASIK. Pachymetric reproducibility on 3D thickness mapping was demonstrated to be 1.3  $\mu\text{m}$  (0.4% to 2%) or better within the central 8-mm zone for epithelium and 5.5  $\mu\text{m}$  (1%) or better for full corneal thickness mapping within the central 4-mm zone.

Degradation in the precision of measurement from single-point to topographic pachymetry is to be expected. Topographic mapping is performed by forming a composite of several scans, the relative corneal position of which may shift by small amounts due to micro-saccadic eye movements during the scanning sequence. Indeed, inspection of the topographic standard deviation maps obtained show

**Table 3**  
**Effect of Speed of Sound on Accuracy of Ultrasound Pachymetry in a Cornea With a Central Epithelial Thickness of 50- $\mu\text{m}$  and a Central Corneal Thickness of 540  $\mu\text{m}$**

Speed of Sound	1610	1640	1670
Corneal Thickness	530	540	550
Error ( $\mu\text{m}$ )	-10	0	+10
% Error	-1.8	0.0	+1.8
Epithelial Thickness	49	50	51
Error ( $\mu\text{m}$ )	-0.9	0	+0.9
% Error	-1.8	0.00	+1.8

*Columns 1 and 3 show the error in corneal and epithelial thickness based upon the maximum theoretical range of speed-of-sound for cornea. A speed-of-sound of 1640 m/s is currently in use. If the speed of sound were 30 m/s higher or lower than the 1640 accepted value, this would produce an error of 10  $\mu\text{m}$  (1.8%) in corneal pachymetry, and an error of 0.9  $\mu\text{m}$  (1.8%) in epithelial pachymetry.*

that the reproducibility varied more in between than within particular axes of scanning.

The single point pachymetric precision for flap thickness measurements (1.14  $\mu\text{m}$ ) was slightly inferior to that of the epithelium (0.61  $\mu\text{m}$ ) or full corneal thickness (0.71  $\mu\text{m}$ ) in the case described. Although this difference may be statistically non-significant, it could also be due to the lamellar interface itself being ultrasonically less well defined. The interface may have a finite thickness filled with mucopolysaccharide matrix as compared with the sharp saline/epithelial, epithelial/Bowman, or the endothelial/aqueous interfaces. Further reproducibility studies on multiple eyes will further elucidate these observed differences.

Although there is a high degree of single-point pachymetric reproducibility, the true topographical localization of the mapped pachymetric measurements may possess uncertainty because we are using visual axis fixation with the opposite eye as a reference position during scanning. Potential differences in phorias could exist between repeated measurements of the same patient or between patients. Within patients, it is probable that the degree of phoria would be relatively constant between examinations. These issues will also affect the accuracy of the true location of the optical axis within a pachymetric map. Both the topographic positioning and visual axis localization issues are being addressed by designing a fixation target that will be located axially in front of the eye being scanned.

The immersion of the cornea in normal saline at 33° C could in principle lead to changes in epithelial and stromal thickness, which would affect the

concordance between the measurements being made and the true thickness of the tissue layers. Preliminary data from our laboratory has shown that the epithelium could be immersed for at least 45 minutes without showing changes in thickness. The stromal thickness, however, did show a gradual change of 50  $\mu\text{m}$  over the 45 minutes of immersion (1  $\mu\text{m}$  per minute). This stromal thickness alteration, given no change in epithelial thickness, could only be ascribed to the lack of evaporative loss of stromal hydration during immersion.<sup>23</sup> The need to perform immersion studies of this nature in a short timeframe should therefore be noted. In this study, data for the 10 corneal thickness maps obtained for patient #2 were acquired with the eye immersed for a period of approximately 10 minutes. General inspection of the 10 epithelial and the 10 corneal thickness maps in Figure 6 shows no apparent sequential increase in thickness.

The accuracy of measurement is defined as the concordance between the measured and the true value. To test the accuracy of measurement by our system, it would be necessary to test it against a system that would be capable of measuring epithelium and flap thickness with greater accuracy in order to deduce the concordance. This was not one of the aims of the current study, but would be of great interest to perform. It is, however, possible to examine the accuracy of ultrasonic measurements from a theoretical standpoint. The accuracy of ultrasonic measurements is, for the most part, a function of the speed-of-sound conversion factor used to determine thickness from a time-based separation in echoes. We can perform an accuracy error analysis based upon the known speed of sound in cornea (1640 m/s) and the maximum theoretical limits of this speed-of-sound. Given that saline possesses a speed of sound of 1532 m/s<sup>20</sup>, it is unlikely that the epithelium could possess a speed-of-sound of less than 1610 m/s at the lower extreme. Given that cartilage possesses a speed of sound of approximately 1668 m/s (at 50 MHz; extrapolated from 1568 m/s at 25 MHz)<sup>24</sup>, it is unlikely that the epithelium could possess a speed-of-sound of more than 1670 m/s at the upper extreme. Given these range limits for the speed of sound, it is possible to perform a theoretical error analysis and hence derive an idea for the accuracy limits of corneal ultrasonic pachymetry. For epithelium, the maximum theoretical pachymetric error would be 0.9  $\mu\text{m}$  for a 50- $\mu\text{m}$  epithelium (1.8%), and for full corneal thickness measurements the maximum error would be 10  $\mu\text{m}$  in a 540- $\mu\text{m}$  cornea (1.8%). It is important to note that the accuracy error due to speed-of-sound inaccuracy

in ultrasound pachymetry will always be constant. Table 3 summarizes these theoretical accuracy error limits for VHF ultrasound corneal pachymetry.

Initial PRK trials over 10 years ago demonstrated a large discrepancy between the calculated theoretical ablation profiles and the effective required profiles to produce a specified refractive change in the cornea. Indeed, Munnerlyn and colleagues<sup>25</sup> originally stated that the calculated ablation profiles depended on having no change in the epithelial thickness profile after healing. This discrepancy has been experimentally found to be greater when correcting myopia using smaller rather than larger ablation zones. We now know that at least part of this regression is due to epithelial changes—especially central hyperplasia—producing a regression of the laser recontouring of the stromal surface.<sup>26,27</sup> The observed clinical results of PRK and LASIK demonstrate an order of magnitude in discrepancy between the cutting accuracy of the excimer laser and the observed accuracy of the refractive procedure; a single pulse of excimer laser energy at a fluence of 192 mJ/mm<sup>2</sup> will photoablate approximately 0.25- $\mu\text{m}$  of stromal tissue.<sup>1</sup> Within a 6-mm zone, a spherical keratectomy would theoretically be 12  $\mu\text{m}$  in depth centrally, to produce corneal flattening equivalent to 1.00 D in refraction. Thus, theoretically, 48 pulses (12  $\div$  0.25) would be required for 1.00 D of flattening, or each pulse would flatten the cornea by approximately 1/48th of a diopter. Current state-of-the-art results of LASIK (or PRK) demonstrate a standard deviation of post-operative refraction of approximately 0.50 to 1.00 D and thus a range of up to 4.00 D from target refraction. Accordingly, the surgical accuracy with which the excimer laser is capable of changing refraction is effectively degraded by two orders of magnitude (4 diopters clinically vs. 1/48th of a diopter cutting accuracy). Therefore, it would be reasonable to propose that only a small proportion of the inaccuracy of LASIK is due to inaccuracy in the laser re-profiling aspects of the procedure and that other factors, such as epithelial remodeling and/or bio-mechanical changes, play the more significant role in the discrepancy.

Several studies have demonstrated a poor correlation between preoperative and postoperative central corneal pachymetry and the planned depth of ablation<sup>28</sup>, and this has hampered our ability to determine the true ablation rates in human cornea *in vivo*. The observed discrepancy is now known to be due, at least in part, to the epithelial changes occurring in the central cornea. As we have demonstrated in this report, by enabling the stroma to be

measured separately from the epithelium, preoperative and postoperative topographically determined thickness data can be subtracted to determine the volume of tissue effectively removed from the cornea. Thus, stromal ablation rates can be measured, notwithstanding the possibility of new stromal tissue deposition in the interface or a change in stromal lamellar density following LASIK. Furthermore, if there were to be topographical variability in the ablation rate (as could occur with differential drying of the stromal bed during ablation, as is thought to occur in the formation of central islands), this would be theoretically detectable. The determination of ablation rates is important not only for improving the accuracy of refractive outcome but also for the safety of LASIK with respect to residual stromal bed thickness limits.

Preliminary data suggest that central epithelial thickness changes significantly after PRK<sup>29</sup>, and recently it was observed that this also occurs after LASIK, despite there being no surgical alteration of the epithelial layer.<sup>5,7,12,30</sup> Lohmann and colleagues, using a hand-held 50 MHz probe, detected epithelial changes that correlated with myopic regression after LASIK.<sup>7</sup> Epithelial thickening changes recorded in the present study (Fig 7, map 7) 6 months after LASIK occurred in a zone confined to the central zone from which tissue was removed from the cornea (the Nidek ablation zone possessed an outer limit of 7.5 mm). Despite the dramatic change observed in the epithelial thickness profile, the refractive result for the left eye of this patient was excellent (uncorrected visual acuity of 20/16, refraction of plano). This supports directly the hypothesis that epithelial changes form part of currently employed nomograms in LASIK, with this particular eye having healed to the exact average level for that specific refraction treated.

Preliminary data from our laboratory suggest that refractively significant corneal profile changes due to epithelial healing do occur after LASIK.<sup>30</sup> We are currently studying epithelial dynamics relative to the surgically induced stromal profile change. It is conceivable that if epithelial power changes follow a biologically confined range of behavior, they may be useful in nomogram adjustment for improved refractive outcomes; preoperative epithelial power determination could then be used to improve the accuracy of LASIK.

The presence of an increase in stromal layer thickness within an annular zone lying outside of the keratectomy (the 8 to 9 mm annulus) is intriguing (c.f. Fig 7: map 8). This finding is consistent with the hypothesis proposed by Dupps and co-workers<sup>31</sup>,

that a retraction of corneal lamellae occurs toward the limbus following the cutting of the corneal lamellae by the microkeratome and laser ablation, more centrally. This retraction could theoretically produce an increase in thickness by the re-refraction of corneal lamellae, and bulging of the peripheral cornea (see Editorial in this issue, pages 407-413). The hypothesis goes on to propose this as further proof of refractive inaccuracy in LASIK (and PRK). This concept is supported not only by our finding of increased peripheral stromal thickness, but by our finding that over this zone there was compensatory epithelial thinning—which would result from an increase in anterior curvature in that annular zone.

Current evaluation of keratome technology relies on either eye bank studies, or the measurement of corneal thickness with a hand-held pachymeter before and after the raising of a flap. Neither of these methods can provide the true central thickness of a flap since ultrasound probe positioning, trauma, edema, and drying at the time of the keratectomy will limit the accuracy of measurement.<sup>32</sup> By utilizing the preoperative intact epithelial component and the postoperative intact stromal component of the flap—after surgical trauma has healed and the edema has cleared—we produced a composite of the original flap profile. We have thus demonstrated a technique with which to determine the true anatomy of the flap and hence the performance of the keratome. The ability to determine the 3D profiles and regional variability of flap thickness by VHF ultrasound B-scanning is important if keratome performance is to be characterized accurately in the human eye *in vivo*. In addition, it is of paramount importance to understand the maximum depth characteristics of each particular keratome to avoid unplanned, excessive thinning of the residual stromal bed after LASIK. The ability to accurately determine the preoperative stromal thickness is an important factor in deciding whether a patient, given his or her amount of myopic refractive error, is an appropriate candidate for LASIK.

The preoperative prediction of the thickness of the residual stromal layer in a particular eye is based on preoperative corneal thickness, highest myopic meridian of refraction, and the intended depth of keratectomy. Preliminary work based on a cohort of eyes before and after LASIK, with 3D VHF thickness mapping, demonstrated that the combined standard deviation of uncertainty in our ability to predict the thickness of the residual stromal layer preoperatively is on the order of 30  $\mu\text{m}$ .<sup>33</sup> Others have shown a correlation between the

preoperatively predicted residual stromal thickness and changes in the “bulge” of the back surface of the cornea.<sup>34</sup> Reports of iatrogenic keratectasia have begun to appear in the literature<sup>35</sup>, and do not seem to be confined to patients with preoperative high-myopia.<sup>36,37</sup> Given the combined uncertainties in the preoperative accuracy of corneal thickness measurement, the thickness of the flap, and the depth of ablation, it behooves us to distinguish between epithelial and biomechanical changes in the cornea when considering LASIK flap-lift enhancement surgery. Using hand-held ultrasonic pachymetry to determine—after a flap is lifted—whether there is sufficient residual stromal tissue available for enhancement surgery is potentially dangerous. As was demonstrated above on 3D thickness mapping of the residual stromal layer, the thinnest point is not always in the center (Fig 7: map 11). Thus, intraoperative pachymetry of the stromal bed under the flap may be used to confirm that further ablation *cannot* be performed (by finding a residual stromal thickness that would not allow further ablation to leave >250  $\mu\text{m}$ ); however, it *cannot* be used to determine if it is safe to proceed with further ablation.

J.I. Barraquer taught in his 1980 textbook on keratomileusis that to prevent progressive keratectasia in keratomileusis, the corneal cap should not be thicker than 300  $\mu\text{m}$ .<sup>32</sup> Assuming the average cornea has a central thickness of approximately 550  $\mu\text{m}$  Barraquer's statement would translate to leaving a residual stromal thickness of at least 250  $\mu\text{m}$ . The ability to determine residual stromal thickness measurements in a topographic manner can enable the surgeon to improve the safety of surgical planning in LASIK enhancement. For example, a patient whose preoperatively predicted residual stromal thickness was 255  $\mu\text{m}$  and who returned with a postoperative refraction of -1.00 D would not be suitable for enhancement, for that would theoretically leave the eye with less than 250  $\mu\text{m}$  of residual stroma after enhancement. By measuring the residual stromal thickness in this eye, we would be able to determine if in fact there existed more residual stromal tissue than expected (eg, because the flap was thinner than expected) and hence safely plan further surgery. Conversely, a patient with a predicted residual stromal thickness of 270  $\mu\text{m}$  and subsequent LASIK that resulted in a postoperative refraction of -1.00 D would normally qualify for further enhancement surgery. This patient's eye, however, may be unsafe to enhance if it were found on measurement of the residual stromal thickness that

this was only 255  $\mu\text{m}$  (eg, because the flap was 15  $\mu\text{m}$  thicker than expected).

The ability to map corneal layers individually in lamellar corneal surgery should enable us to unravel the contributing elements that comprise our currently employed ablation nomogram. These elements clearly include epithelial and stromal healing dynamics and the depth of the keratectomy, but may also relate to other elements such as individual corneal physical moduli, intraocular pressure, and others.

The surgical correction of asymmetric astigmatism using surface-shape mapping has yielded disappointing results.<sup>38</sup> We have demonstrated that epithelial thickness profiles compensate, albeit in certain cases incompletely, for stromal surface asymmetry. Thus, a cornea with asymmetric astigmatism is unlikely to possess a homogeneous epithelial thickness profile and as such, surface topography would poorly represent the true stromal asymmetry.<sup>5</sup> As noted earlier, a significant difference in refractive indices between epithelium (1.401) and anterior stroma (1.373) exists<sup>9</sup> and we have shown that the epithelial-stromal interface curvature leads to an interface power on the order of diopters.<sup>8</sup> It is therefore reasonable to suggest that neither the use of elevation topography of the corneal surface, 3D wavefront, nor spatially resolved refractometry may be sufficient parameters on which to base the surgical repair of asymmetric astigmatism. The ability to map the epithelial thickness profile, and hence derive the shape of the stromal surface, should provide a needed correction factor for elevation topography or wavefront based ablation profiles in the correction of asymmetric corneas.

Orthopedic surgery was practiced without preoperative and postoperative anatomical imaging until the discovery of X-ray in 1895 by Wilhelm Konrad Roentgen, allowing accurate osseous anatomy to guide surgeons. Perhaps layer-by-layer anatomical imaging and biometry of the cornea will have a similar impact on corneal refractive surgery.

#### REFERENCES

1. Huebscher HJ, Genth U, Seiler T. Determination of excimer laser ablation rate of the human cornea using in vivo Scheimpflug videography. *Invest Ophthalmol Vis Sci* 1996;37:42-46.
2. Goss DA, Grosvenor T. Reliability of refraction—a literature review. *J Am Optom Assoc* 1996;67:619-630.
3. Mrochen M, Kaemmerer M, Seiler T. Wavefront-guided laser in situ keratomileusis: early results in three eyes. *J Refract Surg* 2000;16:116-121.
4. Reinstein DZ, Srivannaboon S, Silverman RH, Coleman DJ. The accuracy of routine LASIK; isolation of biomechanical

- and epithelial factors. *Invest Ophthalmol Vis Sci* 2000;41(suppl):S318.
5. Reinstein DZ, Silverman RH, Sutton HF, Coleman DJ. Very high-frequency ultrasound corneal analysis identifies anatomic correlates of optical complications of lamellar refractive surgery: anatomic diagnosis in lamellar surgery. *Ophthalmology* 1999;106:474-482.
  6. Gauthier CA, Epstein D, Holden BA, Tengroth B, Fagerholm P, Hamberg-Nystrom H, Sievert R. Epithelial alterations following photorefractive keratectomy for myopia. *J Refract Surg* 1995;11:113-118.
  7. Lohmann CP, Reischl U, Marshall J. Regression and epithelial hyperplasia after myopic photorefractive keratectomy in a human cornea. *J Cataract Refract Surg* 1999;25:712-715.
  8. Patel S, Reinstein DZ, Silverman RH, Coleman DJ. The shape of Bowman's layer in the human cornea. *J Refract Surg* 1998;14:636-640.
  9. Patel S, Marshall J, Fitzke FW. Refractive index of the human corneal epithelium and stroma. *J Refract Surg* 1995;11:100-105.
  10. Waring GO III. A cautionary tale of innovation in refractive surgery. *Arch Ophthalmol* 1999;117:1069-1073.
  11. Reinstein DZ, Silverman RH, Coleman DJ. High-frequency ultrasound measurement of the thickness of the corneal epithelium. *Refract Corneal Surg* 1993;9:385-387.
  12. Reinstein DZ, Silverman RH, Trokel SL, Coleman DJ. Corneal pachymetric topography. *Ophthalmology* 1994;101:432-438.
  13. Reinstein DZ, Silverman RH, Rondeau MJ, Coleman DJ. Epithelial and corneal thickness measurements by high-frequency ultrasound digital signal processing. *Ophthalmology* 1994;101:140-146.
  14. Reinstein DZ, Patel S, Silverman RH, Aslanides IM, Coleman DJ. Epithelial lenticular types of human cornea: classification and analysis of influence on PRK. *Ophthalmology* 1995;102(suppl):S156
  15. Reinstein DZ, Silverman RH, Trokel SL, Allemann N, Coleman DJ. High-frequency ultrasound digital signal processing for biometry of the cornea in planning phototherapeutic keratectomy. *Arch Ophthalmol* 1993;111:430-431. [Published erratum appears in *Arch Ophthalmol* 1993;111:926].
  16. Reinstein DZ, Aslanides IM, Silverman RH, Asbell PA, Coleman DJ. High-frequency ultrasound corneal pachymetry in the assessment of corneal scars for therapeutic planning. *Clao J* 1994;20:198-203.
  17. Allemann N, Chamon W, Silverman RH, Azar DT, Reinstein DZ, Stark WJ, Coleman DJ. High-frequency ultrasound quantitative analyses of corneal scarring following excimer laser keratectomy. *Arch Ophthalmol* 1993;111:968-973.
  18. Lazzaro DR, Aslanides IM, Belmont SC, Silverman RH, Reinstein DZ, Muller JW, Lloyd HO, Coleman DJ. High frequency ultrasound evaluation of radial keratotomy incisions. *J Cataract Refract Surg* 1995;21:398-401.
  19. Silverman RH, Reinstein DZ, Raevsky T, Coleman DJ. Improved system for sonographic imaging and biometry of the cornea. *J Ultrasound Med* 1997;16:117-124.
  20. Coleman DJ, Woods S, Rondeau MJ, Silverman RH. Ophthalmic ultrasonography. *Radiol Clin North Am* 1992;30:1105-1114.
  21. Najafi DJ, Reinstein DZ, Silverman RH, Coleman DJ. An expert system for corneal layer three dimensional pachymetry. *Invest Ophthalmol Vis Sci* 1997;38(suppl):S920
  22. Segall M, Reinstein DZ, Johnson NF. Computer aided analysis and visualization of high-frequency ultrasound scanning of the human cornea. *IEEE Computer Graphics Applications* 1999;19:74-82.
  23. Solomon R, Silverman RH, Reinstein DZ, Coleman DJ. Ultrasonic corneal pachymetry during immersion in normal hypotonic and hypertonic media in vivo. *Invest Ophthalmol Vis Sci* 1996;37(suppl):S314
  24. Myers SL, Dines K, Brandt DA, Brandt KD, Albrecht ME. Experimental assessment by high frequency ultrasound of articular cartilage thickness and osteoarthritic changes. *J Rheumatol* 1995;22:109-116.
  25. Munnerlyn CR, Koons SJ, Marshall J. Photorefractive keratectomy: a technique for laser refractive surgery. *J Cataract Refract Surg* 1988;14:46-52.
  26. Gauthier CA, Holden BA, Epstein D, Tengroth B, Fagerholm P, Hamberg-Nystrom H. Factors affecting epithelial hyperplasia after photorefractive keratectomy. *J Cataract Refract Surg* 1997;23:1042-1050.
  27. Lohmann CP, Patmore A, Reischl U, Marshall J. The importance of the corneal epithelium in excimer-laser photorefractive keratectomy. *Ger J Ophthalmol* 1996;5:368-72.
  28. Sabetti L, Spadea L, Furcese N, Balestrazzi E. Measurement of corneal thickness by ultrasound after photorefractive keratectomy in high myopia. *J Refract Corneal Surg* 1994;10(suppl):S211-S216.
  29. Reinstein DZ, Aslanides DZ, Silverman RH, Najafi DJ, Brownlow RL, Belmont S, Haight DM, Coleman DJ. Epithelial and corneal 3D ultrasound thickness mapping post excimer laser surgery. *Invest Ophthalmol Vis Sci* 1994;35(suppl):S1739
  30. Srivannaboon S, Reinstein DZ, Sutton HFS, Silverman RH, Holland SP, Coleman DJ. Effect of epithelial changes on refractive outcome in LASIK. *Invest Ophthalmol Vis Sci* 1999;40(suppl):S896
  31. Dupps WJ, Roberts C, Schoessler JP. Peripheral lamellar relaxation: A mechanism of induced corneal flattening in PTK and PRK? *Invest Ophthalmol Vis Sci* 1995;36(suppl):S708
  32. Barraquer JI. *Queratomileusis y queratofakia*. Bogota: Instituto Barraquer de America; 1980.
  33. Reinstein DZ, Srivannaboon S, Sutton HFS, Silverman RH, Holland SP, Coleman DJ. Risk of Ectasia in LASIK: Revised Safety Criteria. *Invest Ophthalmol Vis Sci* 1999;40(suppl):S403.
  34. Wang Z, Chen J, Yang B. Posterior corneal surface topographic changes after laser in situ keratomileusis are related to residual corneal bed thickness. *Ophthalmology* 1999;106:406-410.
  35. Seiler T, Koufala K, Richter G. Iatrogenic keratectasia after laser in situ keratomileusis. *J Refract Surg* 1998;14:312-317.
  36. Geggel HS, Talley AR. Delayed onset keratectasia following laser in situ keratomileusis. *J Cataract Refract Surg* 1999;25:582-586.
  37. Speicher L, Gottinger W. [Progressive corneal ectasia after laser in situ keratomileusis (LASIK)]. *Klin Monatsbl Augenheilkd* 1998;213:247-251.
  38. Wiesinger-Jendritza B, Knorz MC, Hugger P, Liermann A. Laser in situ keratomileusis assisted by corneal topography. *J Cataract Refract Surg* 1998;24:166-174.